AD-A072 879 NAVAL RESEARCH LAB WASHINGTON DC F/G 9/1
THE EQUIVALENT CIRCUIT IN THE MOBILITY ANALOGY OF A MAGNETOSTRI--ETC(U)
MAR 79 S W MEEKS

UNCLASSIFIED NRL-8294 SBIE-AD-E000 305 NL

1 OF 1
AD A072 879

END
DATE FILMED
9-79
DDC

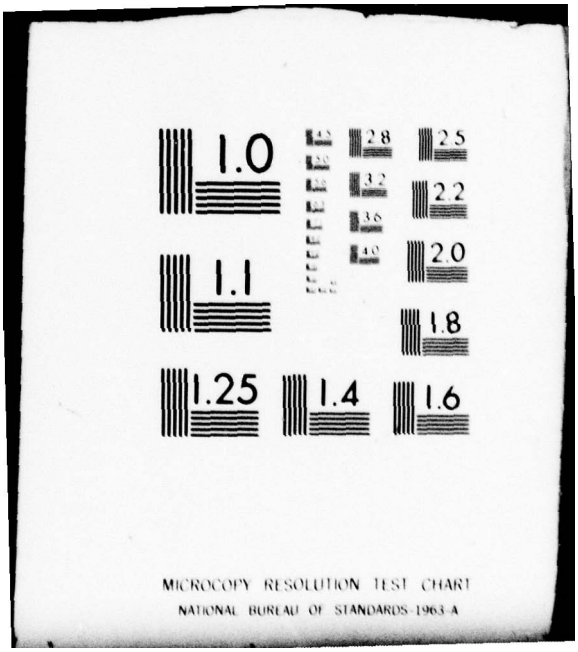
1.0
1.1
1.25
1.4
1.6
2.0
2.2
2.5
2.8
3.2
3.6
4.0
1.8
MICROCOPY RESOLUTION TEST CHART
NATIONAL BUREAU OF STANDARDS-1963-A

NRL Report 8294

The Equivalent Circuit in the Mobility Analogy of a Magnetostrictive Transducer in the Presence of Eddy Currents

STEVEN W. MEEKS

Underwater Sound Reference Detachment
Transducer Branch
P.O. Box 8337
Orlando, Florida 32856

March 26, 1979

NAVAL RESEARCH LABORATORY
Washington, D.C.

SECURITY CLASSIFICATION OF THIS PAGE (When Data Entered)

REPORT DOCUMENTATION PAGE		READ INSTRUCTIONS BEFORE COMPLETING FORM
1. REPORT NUMBER NRL Report 8294	2. GOVT ACCESSION NO.	3. RECIPIENT'S CATALOG NUMBER
4. TITLE (and Subtitle) THE EQUIVALENT CIRCUIT IN THE MOBILITY ANALOGY OF A MAGNETOSTRICTIVE TRANSDUCER IN THE PRESENCE OF EDDY CURRENTS		5. TYPE OF REPORT & PERIOD COVERED Interim report on a continuing NRL Problem. 6. PERFORMING ORG. REPORT NUMBER
7. AUTHOR(s) Steven W. Meeks		8. CONTRACT OR GRANT NUMBER(s)
9. PERFORMING ORGANIZATION NAME AND ADDRESS Underwater Sound Reference Detachment P.O. Box 8337 Orlando, Florida 32856		10. PROGRAM ELEMENT, PROJECT, TASK AREA & WORK UNIT NUMBERS NRL Problem S02-38 Program Element 61153N-11 Project RR011-08
11. CONTROLLING OFFICE NAME AND ADDRESS Department of the Navy Office of Naval Research Arlington, VA 22217		12. REPORT DATE March 26, 1979 13. NUMBER OF PAGES 41
14. MONITORING AGENCY NAME & ADDRESS(if different from Controlling Office)		15. SECURITY CLASS. (of this report) UNCLASSIFIED 15a. DECLASSIFICATION/DOWNGRADING SCHEDULE

16. DISTRIBUTION STATEMENT (of this Report)

Approved for public release; distribution unlimited.

17. DISTRIBUTION STATEMENT (of the abstract entered in Block 20, if different from Report)

18. SUPPLEMENTARY NOTES

19. KEY WORDS (Continue on reverse side if necessary and identify by block number)

Equivalent circuits
Magnetostrictive transducers
Eddy currents

20. ABSTRACT (Continue on reverse side if necessary and identify by block number)

Recent research into the highly magnetostrictive rare earth iron compounds has renewed an interest in magnetostrictive transducers. A typical magnetostrictive transducer is designed with the aid of an equivalent circuit which electrically represents the differential equations that govern the motion of the transducer. The equivalent circuit is used to predict the transmitting responses, receiving response, electrical impedance, and efficiency of the transducer. Ohmic losses generated by eddy currents in metallic magnetostrictive transducers reduce the efficiency and alter the electrical

(Continues)

20. Abstract (Continued)

impedance. Thus an equivalent circuit is required which can predict the effect of eddy currents on the efficiency, the electrical impedance, the transmitting responses, and the receiving response of a magnetostrictive transducer. This report presents the derivation of an equivalent circuit of a magnetostrictive transducer in the presence of eddy currents using an exact eddy-current theory. However, use of the exact theory can be time consuming. Lumped equivalent circuits are also presented which use approximations to the exact theory to simply and accurately predict the efficiency and electrical impedance of a transducer with eddy currents within a frequency range of practical interest near the clamped characteristic frequency.

CONTENTS

THE EQUIVALENT CIRCUIT IN THE MOBILITY ANALOGY OF A MAGNETOSTRICTIVE TRANSDUCER IN THE PRESENCE OF EDDY CURRENTS

INTRODUCTION

Recent research into the highly magnetostrictive rare earth iron compounds has renewed an interest in magnetostrictive transducers. A typical magnetostrictive transducer is designed with the aid of an equivalent circuit. The equivalent circuit is an electrical representation of the differential equations that govern the motion of the transducer. The equivalent circuit is used to predict the transmitting responses, receiving response, electrical impedance, and efficiency of the transducer.

Ohmic losses generated by eddy currents are a primary loss mechanism in metallic magnetostrictive transducers. These ohmic losses reduce the efficiency and alter the electrical impedance of a magnetostrictive transducer. Thus an equivalent circuit is needed which can simply and accurately predict the effect of eddy currents on the efficiency and the electrical impedance of a magnetostrictive transducer.

The active elements of a magnetostrictive transducer are typically in the shape of a thin rod or a stack of thin laminations. For these standard configurations it would be highly desirable to be able to predict the efficiency, receiving and transmitting responses, and electrical impedance as a function of eddy current loss, which is controlled by the rod diameter or lamination thickness.

The first purpose of this report is to show how the equivalent circuit of a magnetostrictive transducer in the presence of eddy currents is derived. Since the equivalent circuit based on the exact theory can be time consuming to use, the second purpose of this report is to present useful approximations to an exact eddy-current theory that can simply and accurately predict the efficienty and electrical impedance of a magnetostrictive transducer in the presence of eddy currents. The third purpose is to discuss the effects of eddy currents on the receiving and transmitting responses of a magnetostrictive transducer. The fourth purpose is to discuss the effect of magnetomechanical coupling on eddy current loss.

THEORY AND DISCUSSION

Eddy Currents in a Rod and a Thin Sheet

When an alternating current is applied to a solenoid, a circumferential electric field is generated by the time-changing flux. If a conducting rod is placed in the solenoid, the electric field generates circumferential currents in the rod (Fig. 1). These currents are in a direc-

Manuscript submitted December 7, 1978.

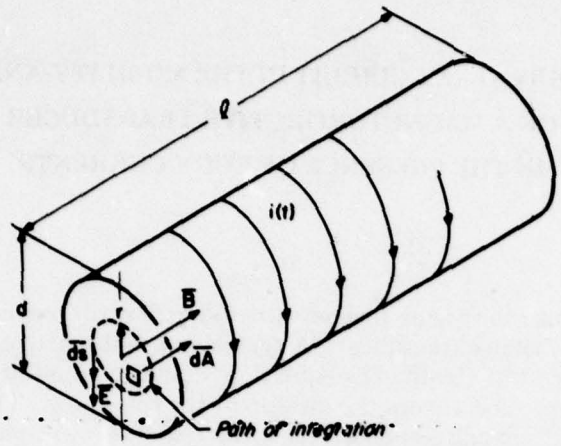

Fig. 1 — Eddy currents in a conducting rod. The current $i(t)$ is increasing with time.

tion so as to generate a magnetic field that opposes the applied magnetic field. These circulating currents are known as eddy currents. In a rod the magnitude of the eddy currents increase in direct proportion to the radial distance from the center of the rod. Thus near the center of the rod the opposing magnetic field generated by the eddy currents is the largest, since all the eddy currents encircle this axis. This effectively shields the center of the rod from the applied magnetic field, leading to the well known *skin effect*. Since the rod in the solenoid has a finite resistivity, the eddy currents also generate an ohmic loss. The shielding effect and ohmic loss generated by the circulating eddy currents alter the electrical impedance of a solenoid with a metallic core. This subsection will present the derivation of the electrical or blocked impedance of a solenoid with a core composed of a rod or a thin sheet in the presence of eddy currents.

The penetration of a magnetic field into a conductor is governed by Maxwell's equations:

$$\nabla \times \mathbf{H} = \mathbf{j} + \frac{\partial \mathbf{D}}{\partial t}\,, \tag{1}$$

where the current density $\mathbf{j} = \sigma\mathbf{E}$ (σ is the conductivity). Equation (1) can be written in time-varying form as

$$\nabla \times \mathbf{H} = (\sigma + j\omega\epsilon)\mathbf{E}. \tag{2}$$

Since this report deals with good conductors at low frequencies, $\omega\epsilon$ is much less than σ and can be neglected. This assumption amounts to neglecting displacement current in comparison with conduction current. Thus one has

$$\nabla \times \mathbf{H} = \sigma\mathbf{E}\,, \tag{3}$$

and taking the curl of each side yields

$$\nabla \times \nabla \times \mathbf{H} = \nabla(\nabla \cdot \mathbf{H}) - \nabla^2\mathbf{H} = \nabla \times \sigma\mathbf{E}\,. \tag{4}$$

Also,

$$\nabla \cdot \mathbf{B} = 0 \tag{5}$$

or

$$\mu(\nabla \cdot \mathbf{H}) = 0, \tag{6}$$

if homogeneity of permeability μ is assumed. Therefore, substituting Eq. (6) into Eq. (4), one has

$$-\nabla^2\mathbf{H} = \sigma(\nabla \times \mathbf{E}) \tag{7}$$

or

$$-\nabla^2\mathbf{H} = \sigma\left(-\frac{\partial \mathbf{B}}{\partial t}\right), \tag{8}$$

since

$$\nabla \times \mathbf{E} = -\frac{\partial \mathbf{B}}{\partial t}\,. \tag{9}$$

Hence the differential equation governing the penetration of a magnetic field into a conductor is

$$\nabla^2\mathbf{H} = \frac{\mu}{\rho}\frac{\partial \mathbf{H}}{\partial t}, \tag{10}$$

where ρ is the resistivity and the permeability is independent of time. Equation (10) can be written in cylindrical coordinates as

$$\nabla^2\mathbf{H} = \mathbf{a}_r\left(\nabla^2\mathbf{H}_r - \frac{2}{r^2}\frac{\partial H_\phi}{\partial \phi} - \frac{H_r}{r^2}\right) + \mathbf{a}_\phi\left(\nabla^2 H_\phi + \frac{2}{r^2}\frac{\partial H_r}{\partial \phi} - \frac{H_\phi}{r^2}\right) + \mathbf{a}_z\left(\nabla^2 H_z\right)$$

$$= \frac{\mu}{\rho}\left[\frac{\partial H_r}{\partial t}\mathbf{a}_r + \frac{\partial H_\phi}{\partial t}\mathbf{a}_\phi + \frac{\partial H_z}{\partial t}\mathbf{a}_z\right]$$

$$= \frac{\mu}{\rho}\frac{\partial \mathbf{H}}{\partial t}\,. \tag{11}$$

For a long thin solenoid with a rod-shaped core and with its long axis in the z direction the following conditions are true:

$$\nabla^2 H_r = \frac{\partial H_\phi}{\partial \phi} = H_r = \nabla^2 H_\phi = \frac{\partial H_r}{\partial \phi} = H_\phi = \frac{\partial H_\phi}{\partial t} = \frac{\partial H_r}{\partial t} = 0. \tag{12}$$

Thus Eq. (11) reduces to

$$\nabla^2 H_z = \frac{\mu}{\rho} \frac{\partial H_z}{\partial t} \tag{13}$$

and with the Laplacian written in cylindrical coordinates is

$$\frac{1}{r} \frac{\partial}{\partial r}\left(r \frac{\partial H_z}{\partial r}\right) + \frac{1}{r^2} \frac{\partial^2 H_z}{\partial \phi^2} + \frac{\partial^2 H_z}{\partial z^2} = \frac{\mu}{\rho} \frac{\partial H_z}{\partial t}. \tag{14}$$

But for a long thin solenoid

$$\frac{\partial^2 H_z}{\partial \phi^2} = \frac{\partial^2 H_z}{\partial z^2} = 0. \tag{15}$$

Thus the differential equation governing the penetration of an alternating magnetic field into a rod contained within a long thin solenoid is

$$\frac{1}{r} \frac{\partial}{\partial r}\left(r \frac{\partial H_z}{\partial r}\right) = \frac{\mu}{\rho} \frac{\partial H_z}{\partial t}. \tag{16}$$

The solution of Eq. (16) is given by Scott [1] as

$$H_z(r) = H_s \left[\frac{\operatorname{ber}\left(\frac{2\theta r}{d}\right) + j \operatorname{bei}\left(\frac{2\theta r}{d}\right)}{\operatorname{ber} \theta + j \operatorname{bei} \theta} \right], \tag{17}$$

where r is the radial distance from the cylinder axis to the point in question, d is the diameter of the rod, and H_s is the magnetic field intensity at the surface of the rod. The parameter θ is given by

$$\theta = \pi d \left(\frac{\mu f}{2\pi \rho}\right)^{\frac{1}{2}}, \tag{18}$$

where μ, ρ, and f are the rod's incremental permeability, resistivity, and frequency respectively in the International System of Units (SI units). The functions ber and bei of Eq. (17) are the real and imaginary portions of the zeroth-order Bessel function of the first kind respectively and have been tabulated [2].

Define a characteristic frequency f_c by setting the parameter $\theta = 1$. Solving for f_c yields

$$f_c = \frac{2\rho}{\pi d^2 \mu} . \tag{19}$$

To examine the physical significance of f_c, solve Eq. (17) for the magnitude of $H_z(0)/H_s$ (that is, let $r = 0$, which is the center of the rod) when $\theta = 1$, which corresponds to $f = f_c$. This yields $H_z(0)/H_s = 0.985$. Thus the magnetic field at the center of the rod is 98.5% of its value at the surface at $f = f_c$. Therefore f_c corresponds to the frequency for a given diameter, permeability, and resistivity below which the penetration of flux into the rod is essentially uniform.

The electrical impedance of the rod is

$$Z = j\omega L = j\omega \frac{N\phi}{I} = \frac{j\omega N \int_A B_z(r)\, dA}{I} , \tag{20}$$

where $B_z(r) = \mu H_z(r)$. If one carries out the integration indicated by Eq. (20), the result is

$$Z = j\omega L_0 \left[\frac{2}{\theta} \left(\frac{\text{ber}\,\theta\ \text{bei}'\,\theta - \text{bei}\,\theta\ \text{ber}'\,\theta}{\text{ber}^2\,\theta + \text{bei}^2\,\theta} \right) - j \frac{2}{\theta} \left(\frac{\text{ber}\,\theta\ \text{ber}'\,\theta + \text{bei}\,\theta\ \text{bei}'\,\theta}{\text{ber}^2\,\theta + \text{bei}^2\,\theta} \right) \right] , \tag{21}$$

where

$$L_0 = \frac{N^2 A \mu}{\ell} . \tag{22}$$

With the aid of

$$\theta = \left(\frac{f}{f_c} \right)^{\frac{1}{2}} , \tag{23}$$

$$\chi_R = \frac{\mu'}{\mu} = 2 \left(\frac{f_c}{f} \right)^{\frac{1}{2}} \left[\frac{\text{ber}\left(\frac{f}{f_c} \right)^{\frac{1}{2}} \text{bei}'\left(\frac{f}{f_c} \right)^{\frac{1}{2}} - \text{bei}\left(\frac{f}{f_c} \right)^{\frac{1}{2}} \text{ber}'\left(\frac{f}{f_c} \right)^{\frac{1}{2}}}{\text{ber}^2\left(\frac{f}{f_c} \right)^{\frac{1}{2}} + \text{bei}^2\left(\frac{f}{f_c} \right)^{\frac{1}{2}}} \right] , \tag{24}$$

and

$$\chi_I = \frac{\Delta R}{2\pi f L_0} = 2\left(\frac{f_c}{f}\right)^{\frac{1}{2}} \left[\frac{\mathrm{ber}\left(\frac{f}{f_c}\right)^{\frac{1}{2}} \mathrm{ber}'\left(\frac{f}{f_c}\right)^{\frac{1}{2}} + \mathrm{bei}\left(\frac{f}{f_c}\right)^{\frac{1}{2}} \mathrm{bei}'\left(\frac{f}{f_c}\right)^{\frac{1}{2}}}{\mathrm{ber}^2\left(\frac{f}{f_c}\right)^{\frac{1}{2}} + \mathrm{bei}^2\left(\frac{f}{f_c}\right)^{\frac{1}{2}}} \right], \tag{25}$$

Eq. (21) can be rewritten as

$$Z = j\omega L_0(\chi_R - j\chi_I) = \omega L_0 \chi_I + j\omega L_0 \chi_R . \tag{26}$$

The terms χ_R and χ_I are the real and imaginary parts of an eddy current factor χ for a rod. Equation (26) can be alternatively written as

$$Z = j\omega L_0 \chi = j\omega L_0 \chi_0 e^{j\zeta}, \tag{27}$$

where

$$\chi_0 = \left(\chi_R^2 + \chi_I^2\right)^{\frac{1}{2}}$$

and

$$\zeta = \tan^{-1}\left(\frac{\chi_I}{\chi_R}\right).$$

Thus the electrical impedance can be viewed as an inductor of value $L_0\chi$. The complex eddy-current factor χ may be attached to the permeability in L_0, thus accounting for eddy currents by viewing the permeability as complex. The derivation of χ_R and χ_I is originaliy due to Scott [1]. The expressions for χ_R and χ_I can be found in both Bozorth [3] and Scott [1].

The permeability μ' in Eq. (24) is the "apparent permeability"; that is, it is the permeability which the magnetic field sees in the presence of eddy currents. The permeability μ in Eq. (24) is the limiting value of μ', approached at low frequencies. The ΔR in Eq. (25) is the difference between the measured alternating-current resistive component of the impedance R and the direct-current resistance R_0. The difference ΔR is caused by eddy currents. The inductance L_0 in Eq. (22) or (25) is the limiting value of the measured inductance approached at low frequencies. Figure 2 shows plots of χ_R, χ_I, χ_0, and ζ. Several useful approximations to χ_R, χ_I, and ζ for high and low f/f_c are also shown in Fig. 2. The use of Eq. (24) and Fig. 2 shows that the "apparent permeability" μ' is a decreasing function of frequency.

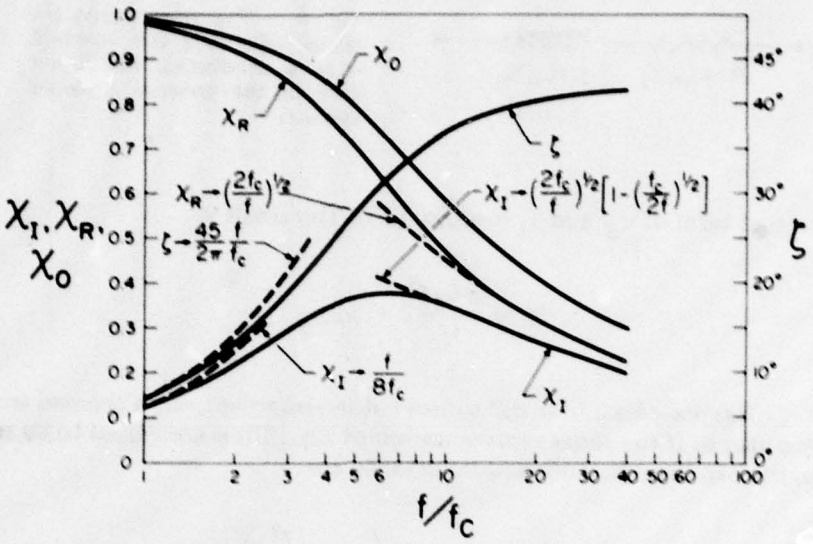

Fig. 2 — Eddy current components for a rod

From Eq. (26) it is seen that in the presence of eddy currents the electrical impedance takes on a resistive component which is proportional to χ_I. The physical significance of the resistive component is that it is the energy-dissipating mechanism of the eddy currents. It is also seen that the imaginary portion of the impedance is proportional to χ_R. This results in a reduction in the inductance as a function of frequency. This observation is consistent with the decrease in the "apparent permeability" as frequency increases. The equivalent circuit of the electrical impedance of a long thin solenoid with a conducting rod-shaped core in the presence of eddy currents is shown in the general case in Fig. 3.

The exact equivalent circuit shown in Fig. 3 is inconvenient to use, because both R and L depend on frequency. A much more convenient expression is a lumped equivalent circuit in which none of the components vary with frequency. This can be derived by considering the expressions for χ_R and χ_I given by Bozorth [3] for a rod when $f < f_c$:

$$\chi_R = 1 - \frac{1}{48}\left(\frac{f}{f_c}\right)^2 + \frac{19}{30{,}720}\left(\frac{f}{f_c}\right)^4 + \ldots \tag{28}$$

and

$$\chi_I = \frac{1}{8}\left(\frac{f}{f_c}\right) - \frac{11}{3{,}072}\left(\frac{f}{f_c}\right)^3 + \frac{473}{4{,}343{,}680}\left(\frac{f}{f_c}\right)^5 + \ldots . \tag{29}$$

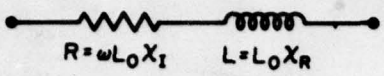

Fig. 3 — The exact equivalent circuit of a long thin solenoid with a conducting rod-shaped core in the presence of eddy currents

Substitute the first term of χ_R and χ_I into Eq. (26). The result is

$$Z \approx \frac{\pi L_0 f^2}{4 f_c} + j\omega L_0 \tag{30}$$

for $f/f_c < 1$. This representation is still somewhat inconvenient, since the real term depends on frequency squared. If the series representation of Eq. (30) is converted to its equivalent parallel form, the parallel resistance and inductance are

$$R_p = 16\pi f_c L_0 \left(1 + \frac{f^2}{64 f_c^2}\right) \tag{31}$$

and

$$L_p = L_0 \left(1 + \frac{f^2}{64 f_c^2}\right). \tag{32}$$

When $f < f_c$, the term $f^2/64f_c^2$ can be neglected with an error of less than 2%. Thus the lumped equivalent circuit of a conducting rod in the presence of eddy currents shown in Fig. 4 is obtained. The characteristic frequency f_c in Fig. 4 is given by Eq. (19).

A derivation analogous to the one that leads to Fig. 3 can be performed for a conducting core composed of thin laminated sheets. Only the results will be presented here. The original derivation can be found in Ref. 1. The eddy current components for a thin sheet are given by Scott [1] and Bozorth [3] and are

$$\chi_R = \frac{\mu'}{\mu} = \left(\frac{f_c}{2f}\right)^{\frac{1}{2}} \frac{\sinh\left(\frac{2f}{f_c}\right)^{\frac{1}{2}} + \sin\left(\frac{2f}{f_c}\right)^{\frac{1}{2}}}{\cosh\left(\frac{2f}{f_c}\right)^{\frac{1}{2}} + \cos\left(\frac{2f}{f_c}\right)^{\frac{1}{2}}} \tag{33}$$

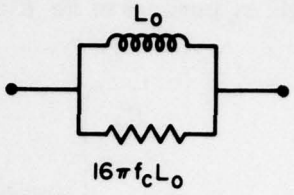

Fig. 4 — The approximate equivalent circuit of a solenoid with a conducting rod-shaped core in the presence of eddy currents for $f < f_c$

and

$$\chi_I = \frac{\Delta R}{2\pi f L_0} = \left(\frac{f_c}{2f}\right)^{\frac{1}{2}} \frac{\sinh\left(\frac{2f}{f_c}\right)^{\frac{1}{2}} - \sin\left(\frac{2f}{f_c}\right)^{\frac{1}{2}}}{\cosh\left(\frac{2f}{f_c}\right)^{\frac{1}{2}} + \cos\left(\frac{2f}{f_c}\right)^{\frac{1}{2}}} . \tag{34}$$

In Eqs. (33) and (34)

$$f_c = \frac{2\rho}{\pi t^2 \mu} , \tag{35}$$

where ρ is the resistivity in ohm-meters, t is the thickness in meters, and μ is the permeability in SI units. The characteristic frequency for the case of a thin sheet again means the frequency below which the penetration of flux into a sheet is essentially uniform. Plots of χ_R, χ_I, χ_0, and ζ versus f/f_c can be found in Ref. 4. The exact equivalent circuit of the electrical impedance of a long thin solenoid with a conducting core composed of thin laminations in the presence of eddy currents is also given by Fig. 3, with Eqs. (33) and (34) now applying to χ_R and χ_I.

An approximation to the exact equivalent circuit of a long thin solenoid with a core composed of thin sheets has been obtained in Ref. 4. The approximate equivalent circuit is similar to Fig. 4 except that the resistance is $6\pi f_c L_0$, where f_c is given by Eq. (35).

The complex impedance of the equivalent circuit shown in Fig. 4 is

$$Z_c = \frac{16\pi f_c \omega^2 L_0}{\omega^2 + (16\pi f_c)^2} + j\left[\frac{(16\pi f_c)^2 \omega L_0}{\omega^2 + (16\pi f_c)^2}\right]. \tag{36}$$

Let the real and imaginary portions of Eq. (36) equal R_c and X_c respectively. Thus

$$\left.\frac{R_c}{\omega_c L_0}\right|_{\substack{\text{equivalent}\\ \text{circuit}}} = \frac{8\left(\frac{f}{f_c}\right)^2}{\left(\frac{f}{f_c}\right)^2 + 64} \tag{37}$$

and

$$\left.\frac{X_c}{\omega_c L_0}\right|_{\substack{\text{equivalent}\\ \text{circuit}}} = \frac{64\left(\frac{f}{f_c}\right)}{\left(\frac{f}{f_c}\right)^2 + 64}. \tag{38}$$

The exact expressions for $R_c/\omega_c L_0$ and $X_c/\omega_c L_0$ are given by the real and imaginary portions respectively of Eq. (26) normalized to $\omega_c L_0$:

$$\left.\frac{R_c}{\omega_c L_0}\right|_{\substack{\text{exact}\\ \text{theory}}} = \frac{fx_I}{f_c} \tag{39}$$

and

$$\left.\frac{X_c}{\omega_c L_0}\right|_{\substack{\text{exact}\\ \text{theory}}} = \frac{fx_R}{f_c}. \tag{40}$$

Figure 5 is a comparison of the loci of points predicted by Eqs. (37) and (38) (the equivalent circuit of Fig. 4) and those predicted by Eqs. (39) and (40) (the exact equivalent circuit of Fig. 3). The loci of the impedance of the lumped equivalent circuit describes an arc of a circle (the lower curve in Fig. 5) which agrees within 1% with the exact equivalent circuit up to $f = f_c$. Deviations begin above $f = f_c$ (particularly in the resistance), but agreement is still fair at $3f_c$ and usable up to $f = 4f_c$. The loci of the impedance of a lossless inductor, if plotted on Fig. 5, would appear as a straight line on the ordinate with the frequency scale increasing upward.

The comparison of the exact and approximate equivalent circuits for a core composed of a stack of thin laminated sheets is given in Ref. 4. In this case the approximate equivalent circuit is usable up to $f = 2f_c$.

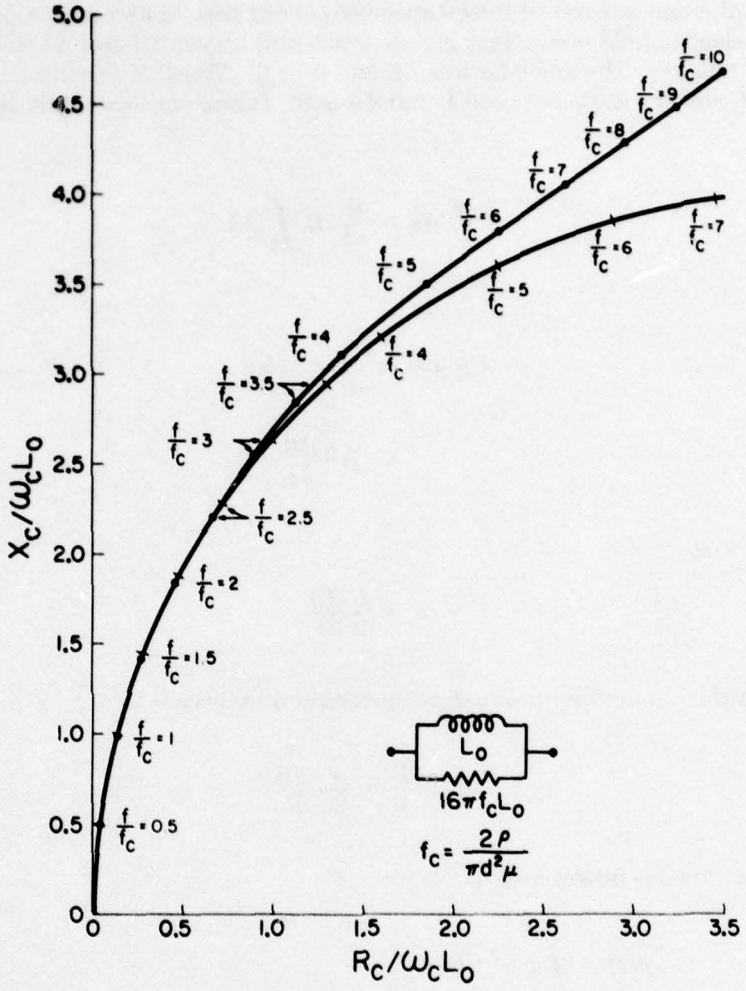

Fig. 5 — The normalized theoretical components of the impedance of a core composed of a rod (upper curve) and the normalized components of the impedance of the equivalent circuit shown (lower curve)

An enlightening alternate derivation of the equivalent circuit of Fig. 4 can be obtained through use of Faraday's law. Consider Fig. 1, which shows a conducting rod in the presence of an alternating magnetic flux. Assume that the flux density is increasing and uniform across the cross-sectional area of the rod. This assumption means that the rod is very long and that the frequency is below the characteristic frequency. Faraday's law relates the time-changing magnetic flux to the electric field produced for a fixed region in space:

$$-\oint \mathbf{E} \cdot \mathbf{ds} = \frac{d}{dt} \int_A \mathbf{B} \cdot \mathbf{da}. \tag{41}$$

Now perform the line integral of the electric field about the circular path a distance r from the axis. The electric field is constant in magnitude and tangential around this path due to the circular symmetry. The angle between E and ds is 0°. The flux density B is also uniform across the rod, and the angle between B and dA is 0°. If one considers only the magnitude, then

$$E \oint ds = \frac{d}{dt} B \int_A dA. \tag{42}$$

Thus

$$E\, 2\pi r = \frac{d}{dt}(\pi r^2 \mathrm{B}) \tag{43}$$

$$= \pi r^2 \frac{dB}{dt}, \tag{44}$$

which implies that

$$E = \frac{r}{2} \frac{dB}{dt}. \tag{45}$$

The density of the circumferential surface current at a radius r is

$$J = \frac{E}{\rho} = \frac{r}{2\rho} \frac{dB}{dt}. \tag{46}$$

The total instantaneous power lost is

$$p(t) = \oint_v \rho J^2 \, dv \tag{47}$$

$$= \int_{z=0}^{\ell} \int_{\theta=0}^{2\pi} \int_{r=0}^{\frac{d}{2}} \rho \frac{r^2}{4\rho^2} \left(\frac{dB}{dt}\right)^2 r \, dr d\theta dz, \tag{48}$$

which yields

$$p(t) = \frac{\pi d^2 \ell}{4} \frac{d^2}{32\rho} \left(\frac{dB}{dt}\right)^2, \tag{49}$$

where $\frac{\pi d^2 \ell}{4}$ is the volume of the rod. Let A equal the area of the rod; then

$$p(t) = \frac{A\ell d^2}{32\rho}\left(\frac{dB}{dt}\right)^2 . \tag{50}$$

The voltage induced in the coil is

$$e(t) = NA\frac{dB}{dt} . \tag{51}$$

Solving Eq. (51) for $(dB/dt)^2$ yields

$$\left(\frac{dB}{dt}\right)^2 = \frac{e^2(t)}{N^2A^2} . \tag{52}$$

Substituting Eq. (52) into Eq. (50) yields

$$p(t) = \frac{d^2e^2(t)\ell}{32\rho N^2 A} = \frac{e^2(t)}{R} , \tag{53}$$

which implies that

$$R = \frac{32\rho N^2 A}{d^2\ell} \text{ ohms.} \tag{54}$$

The resistance given by Eq. (54) is identical to the resistance $16\pi f_c L_0$ shown in Fig. 4. Thus both derivations yield the same result for a long rod at frequencies below the characteristic frequency. The resistance $6\pi f_c L_0$ of a thin laminated sheet can be obtained in an analogous manner through use of Faraday's law [5].

Equivalent Circuit of a Magnetostrictive Toroid in the Presence of Eddy Currents

The equivalent circuits presented thus far have had no mention of magnetostriction. This subsection will present the equivalent circuit of a magnetostrictive toroid with a core composed of a circularly cross-sectioned rod or a number of thin laminated sheets in the presence of eddy currents.

The equivalent circuit of a magnetostrictive transducer can be formed in three ways:

- by the mobility analogy,

- by shifting force and velocity by 90°, or
- by F.V. Hunt's space operator.

The effect of eddy currents on the equivalent circuit formed by shifting the force and velocity by 90° is discussed in Refs. 4 and 6. The effect of eddy currents on the equivalent circuit formed by Hunt's space operator is discussed in Ref. 7 along with an enlightening discussion of all three representations in the absence of eddy currents. The equivalent circuits formed by shifting the force and velocity by 90° and formed by Hunt's space operator have the disadvantage of an imaginary frequency-dependent turns ratio, which leads to frequency-dependent mechanical elements even in the absence of eddy currents. The presence of eddy currents further complicates these two equivalent circuits. The mobility analogy is the simplest to use and the most widely accepted representation of electromagnetic transducers. The use of the mobility analogy when eddy currents are present leads to an equivalent circuit that has frequency-independent elements for a certain frequency range, as will be shown.

The equivalent circuit of a magnetostrictive toroid in the mobility analogy without eddy current loss is shown in Fig. 6. This equivalent circuit does not include ohmic loss, which can be accounted for by simply inserting a resistor, whose value is equal to the dc resistance of the coil, in series with the blocked inductance L_0. In the mobility analogy, force is analogous to current, and velocity is analogous to voltage. In this figure, L_0 is the blocked or purely electrical impedance, C_m is the mechanical compliance, M_m is the mechanical mass, $1/R_m$ is the inverse of the mechanical resistance, and $1/R_A$ and M_A compose the radiation mobility of a sphere. The toroid in this report is assumed to be end capped, so that it is a volume expander. At low frequencies the radiation mobility of a sphere is used to approximate the toroid's radiation mobility. The expressions for the equivalent circuit parameters are

$$L_0 = \frac{N^2 A_c \mu_{33}^S}{2\pi r}, \tag{55}$$

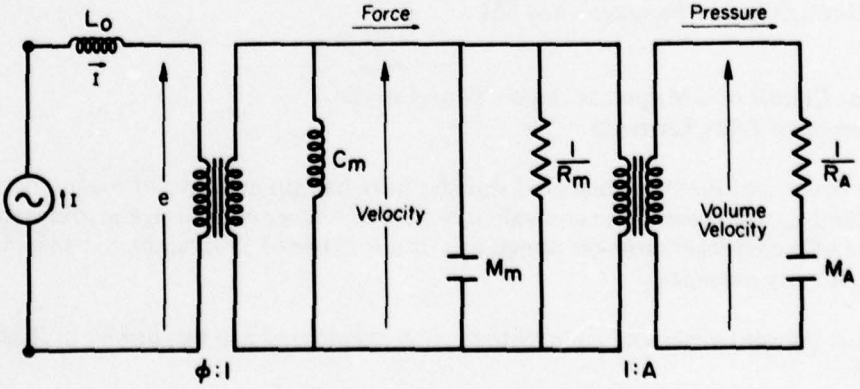

Fig. 6 — The equivalent circuit of a magnetostrictive toroid in the mobility analogy without eddy current loss

$$C_m = \frac{rs_{33}^H}{2\pi A_c}, \tag{56}$$

$$M_m = 2\pi r A_c D, \tag{57}$$

$$R_m = \frac{\omega_0 M_m}{Q_m}, \tag{58}$$

$$\frac{1}{R_A} = \frac{4\pi r_e^2}{d_0 c_0}, \tag{59}$$

and

$$M_A = \frac{d_0}{4\pi r_e}, \tag{60}$$

where

N is the number of turns of wire,

A_c is the cross-sectional area of the metallic core,

μ_{33}^S is the dynamic permeability of the core at a constant strain (the blocked permeability),

r is the radius of the toroid,

D is the density of the core,

s_{33}^H is the elastic compliance coefficient measured at constant magnetic-field intensity,

ω_0 is 2π times the unloaded (in air) resonance frequency,

Q_m is the mechanical Q measured in air,

r_e is the equivalent radius of a sphere which has a surface area equal to the active surface area of the end-capped toroid,

d_0 is the density of water,

c_0 is the speed of sound in water,

ϕ is the electromechanical turns ratio, and

A is the mechanoacoustic turns ratio, which in this case is the active surface area of the toroid.

Eddy currents are accounted for in the equivalent circuit by assuming a complex permeability as suggested by the $L_0\chi$ term of Eq. (27). The eddy current factor χ appears not only in the blocked impedance but also in the electromechanical turns ratio ϕ in the mobility analogy, as will be shown.

The derivation of the electromechanical turns ratio ϕ begins with the magnetostrictive equations of state for a thin rod:

$$S_3 = s^B_{33} T_3 + g_{33} B_3 \tag{61}$$

and

$$H_3 = -g_{33} T_3 + \nu^T_{33} B_3 . \tag{62}$$

If S_3 is set equal to zero, Eq. (61) becomes

$$T_3 = \frac{-g_{33} B_3}{s^B_{33}} . \tag{63}$$

The flux density in the clamped ($S_3 = 0$) toroid is

$$B_3 = \mu^S_{33} \chi H_3 . \tag{64}$$

Here the permeability is complex due to the presence of eddy currents. Substitution of Eq. (64) into Eq. (63) yields

$$T_3 = \frac{-g_{33} \mu^S_{33} \chi H_3}{s^B_{33}} . \tag{65}$$

But $T_3 = \frac{F_3}{A_c}$; therefore

$$F_3 = \frac{-g_{33} \mu^S_{33} \chi A_c H_3}{s^B_{33}} . \tag{66}$$

In a toroid the radial force is related to the circumferential force in the toroid by

$$F_r = 2\pi F_3 . \tag{67}$$

Also, the magnetic field of a toroid is given by

$$H_3 = \frac{NI}{2\pi r}. \tag{68}$$

Substitution of Eqs. (67) and (68) into Eq. (66) yields

$$\frac{F_r}{I} = \frac{-g_{33}\mu_{33}^S \chi A_c N}{r s_{33}^B}. \tag{69}$$

By use of

$$\mu_{33}^S = \mu_{33}^T(1 - k_{33}^2), \tag{70}$$

$$g_{33} = \frac{d_{33}}{\mu_{33}^T}, \tag{71}$$

and

$$s_{33}^B = s_{33}^H(1 - k_{33}^2), \tag{72}$$

the following equation is produced for magnitude only:

$$\frac{F_r}{I} = \frac{N d_{33} A_c \chi}{r s_{33}^H} = \phi \Big|_{\substack{\text{without} \\ \text{eddy currents}}} \cdot \chi. \tag{73}$$

Since the eddy current factor χ is a complex number, the turns ratio F_r/I in Eq. (73) is also a complex number.

The equivalent circuit of Fig. 6 can now be modified to account for eddy current losses by replacing the blocked inductance L_0 by $L_0\chi$ and the electromechanical turns ratio ϕ by $\phi\chi$. Figure 7 shows the equivalent circuit of a magnetostrictive toroid in the presence of eddy currents with the transformers removed. The complex eddy-current factor is reflected in the mechanical mobility and the radiation mobility. If the individual components of Fig. 7 are separated into their real and imaginary portions, Fig. 8 results. Each of the components in Fig. 8 is a complicated function of frequency, due to the eddy current terms. This makes the frequency analysis of the circuit difficult.

To make the analysis of the circuit somewhat simpler, it was necessary to convert the circuit to mechanical units. This is done by moving the electromechanical transformer of Fig. 6 to the left and the mechanoacoustic transformer to the right. The result is shown in Fig. 9. The resistors in Fig. 9 represent inverse mechanical resistances with units of seconds per kilogram. The inductors represent mechanical compliances with units of meters per

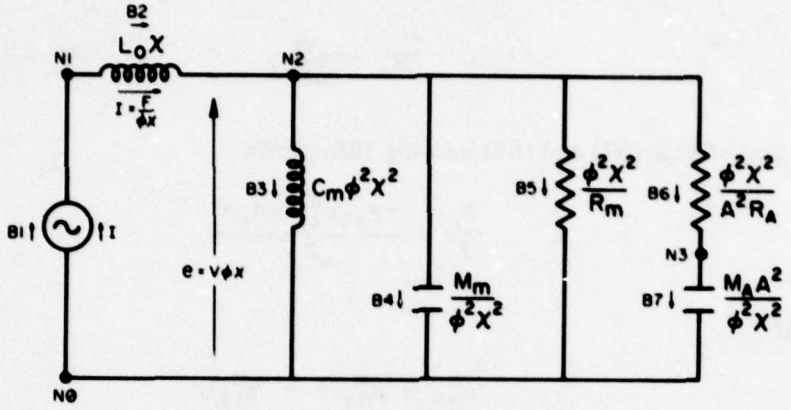

Fig. 7 — The equivalent circuit, in electrical units, of a magnetostrictive toroid in the presence of eddy currents

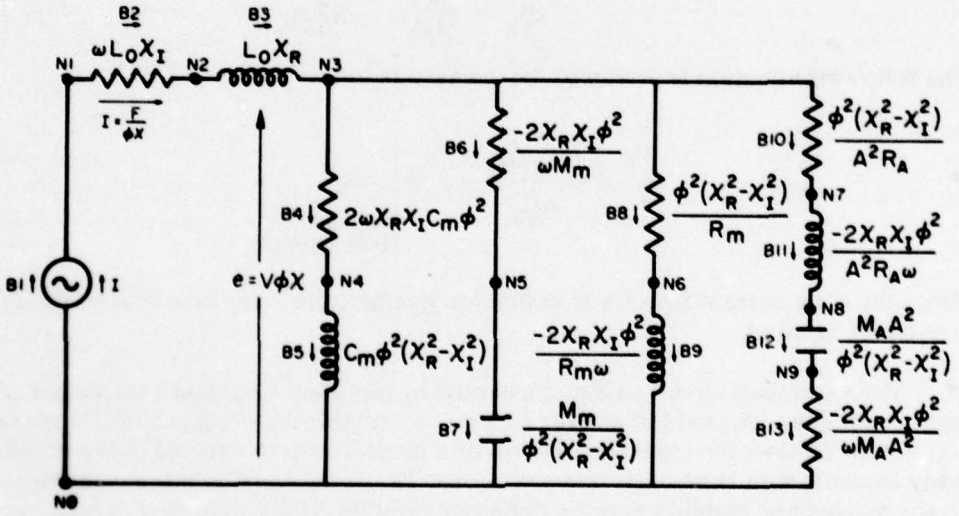

Fig. 8 — The equivalent circuit, in electrical units, of a magnetostrictive toroid in the presence of eddy currents, with individual elements separated into real and imaginary components

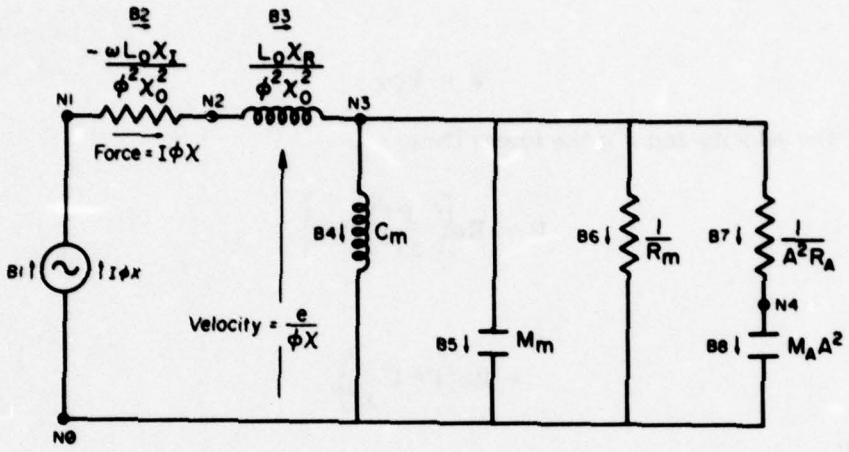

Fig. 9 — The equivalent circuit, in mechanical units, of a magnetostrictiive toroid in the presence of eddy currents

newton. The capacitors represent masses with units of kilograms. The through variable is the force produced by the toroid in newtons. The across variable is the velocity of the toroid in meters per second. The eddy current terms in Fig. 9 are lumped into three components: the two elements of the blocked mechanical mobility (branches 2 and 3 (B2 and B3)) and the force generator (branch 1). The ideal sinusoidal current generator of Fig. 8 has now become a force generator of value $I\phi\chi$ newtons. Figure 2 shows that χ_0 and thus the magnitude of the force generator are decreasing functions of frequency. The decrease in force produced by the magnetostrictive core as a function of frequency is due to the reverse flux generated by the eddy currents. The monotonic decrease of force with frequency may be explained by noting that the eddy currents increase with frequency. Hence the opposing magnetic field increases, thereby resulting in a continual decrease in the net flux that produces the force from the magnetostrictive core.

The equivalent circuit shown in Fig. 9 can now be used to analyze a magnetostrictive transducer in the presence of eddy currents. Figure 9 can be used to calculate the efficiency, transmitting responses, receiving response, and impedance, all as a function of frequency. Before performing the analysis, one must first observe how the power dissipated in the circuit elements of Fig. 9 is calculated.

Power is defined as

$$P = \text{Re}\,(I^* e), \tag{74}$$

where I^* is the complex conjugate of the current and e is the voltage. Figure 9 implies that

$$I^* = \left(\frac{F}{\phi\chi}\right)^* \tag{75}$$

and

$$e = V\phi\chi\,, \tag{76}$$

where V is the velocity and F is the force. Thus

$$P = \mathrm{Re}\left[\left(\frac{F^*}{\phi\chi^*}\right) V\phi\chi\right] \tag{77}$$

$$= \mathrm{Re}\left(F^* V \frac{\chi}{\chi^*}\right). \tag{78}$$

But $F = \frac{V}{Y_m}$; therefore

$$P = \mathrm{Re}\left[\left(\frac{V}{Y_m}\right)^* V\frac{\chi}{\chi^*}\right]\,, \tag{79}$$

where Y_m is the mechanical admittance (mobility), which is equal to the reciprocal of the mechanical impednace. Equation (79) can be written as

$$P = |V|^2\,\mathrm{Re}\left(\frac{e^{-2j\xi}}{Y_m{}^*}\right) \tag{80}$$

with the use of $V^* V = |V|^2$ and $\chi/\chi^* = e^{-2j\xi}$.

Calculation of the efficiency of the transducer depicted by the equivalent circuit of Fig. 9 begins with the force generator whose magnitude is determined by first calculating f/f_c^s for the particular frequency of interest. The frequency f_c^s is the blocked characteristic frequency and is defined by

$$f_c^s = \frac{2\rho}{\pi d^2 \mu_{33}^S} \tag{81}$$

for a rod of circular cross section and by

$$f_c^s = \frac{2\rho}{\pi t^2 \mu_{33}^S} \tag{82}$$

for a thin sheet. The symbols in Eqs. (81) and (82) are the same as in Eqs. (19) and (35) respectively, except μ_{33}^S is the blocked incremental permeability. The blocked characteristic

frequency is required whenever one is dealing with an equivalent circuit, since the eddy current factor (which is written as a series composed of f/f_c^s as in Eqs. (28) and (29)) is attached to the blocked permeability, as in Eq. (64), and to the blocked inductance of Fig. 7. Once f/f_c^s is determined, χ_0 is read from Fig. 2 or from Ref. 4 if a thin sheet is being used. The magnitude of the force generator is thus $I\phi\chi_0$. The phase angle of χ is not put into the force generator, since one is interested in only the magnitude of the velocity, as indicated in Eq. (80). The analysis of Fig. 9 was carried out on a PDP-11/45 computer using an ac-circuit analysis program [8]. The values of the elements were chosen to be numerically equal to their mechanical quantities. The branch voltages and currents were therefore interpreted as velocities and forces respectively. The power dissipated in each element was calculated using the velocity from the circuit analysis program, the phase angle ζ from Fig. 2 or Ref. 4, and Eq. (80). It is not necessary to calculate the power dissipated in the blocked mechanical mobility (branches 2 and 3 of Fig. 9) using the method described. The power dissipated in these elements is

$$P = I^2 \omega L_0 \chi_I, \tag{83}$$

which shows that this power can be determined from known constants and a given frequency.

The steps necessary to perform an efficiency analysis using Fig. 9 are summarized as follows:

1. Calculate f/f_c^s from the desired frequency and Eqs. (81) or (82).

2. Determine χ_0 from Fig. 2 or Ref. 4.

3. Input the value of the force generator ($I\phi\chi_0$) and the values of mechanical compliances, masses, and resistances into an ac-circuit analysis program.

4. Obtain the magnitude of the velocity across each element (except the blocked mechanical mobility) and the phase angle ζ from the graphs to calculate the power dissipated in each element via Eq. (80).

5. Use the power dissipated in the mechanical elements and Eq. (83) to determine the efficiency in the presence of eddy currents:

$$\text{efficiency} = \frac{P_A}{P_M + P_E + P_A}, \tag{84}$$

where P_A is the acoustic power, P_M is the mechanical power, and P_E is the power dissipated by eddy currents.

6. To calculate the efficiency at another frequency, return to step 1 and use the new f/f_c^s to calculate the new magnitude of the force generator. This new value of the force generator is input into the ac-circuit analysis program, and the new power dissipated in each element is calculated from Eq. (80). For each new frequency only one element (the force generator) of Fig. 9 need be changed to calculate the efficiency.

To calculate the transmitting current response, one first calculates the acoustic power dissipated in the mechanical radiation mobility ($1/A^2 R_A$) using the technique described. Then the on-axis acoustic pressure is calculated via

$$p = \frac{1}{r}\left(\frac{P_a d_0 c_0 R_\theta}{4\pi}\right)^{\frac{1}{2}} , \tag{85}$$

where p is the on-axis acoustic pressure, P_a is the acoustic power, d_0 is the density of water, c_0 is the speed of sound in water, and R_θ is the directivity factor. Since the pressure calculated is for a 1-ampere drive (if the I in $I\phi\chi_0$ is set equal to unity), the pressure obtained from Eq. (85) will be the transmitting current response. The free-field voltage sensitivity can be obtained [9] from

$$J = \text{reciprocity parameter} = \frac{M}{S}, \tag{86}$$

where M is the free-field voltage sensitivity and S is the transmitting current response, along with

$$J = \frac{2d}{d_0 f} \times 10^{-12} , \tag{87}$$

in which d is the measurement distance, d_0 is the density of water, and f is the frequency, all in SI units.

To calculate the electrical impedance, one proceeds as follows:

$$\frac{V}{F} = \frac{e}{\phi\chi}\frac{1}{I\phi\chi} = \frac{Z_e}{\phi^2\chi^2} \tag{88}$$

or

$$Z_e = \frac{V}{F}\phi^2\chi^2 = \frac{V}{I}\phi\chi , \tag{89}$$

where V is the velocity and I is the current. Equation (89) can be simplified for calculation by noting that the velocity will contain the phase angle $-\zeta$ when the force generator has the angle $-\zeta$. If one uses only the magnitude of the force generator in the equivalent circuit and adds $-\zeta$ to the phase angle of the resulting velocity, then

$$Z_e = \frac{V}{I}\phi\chi_0 e^{-j2\zeta} , \tag{90}$$

and if $I = 1$ ampere and $V = |V|e^{j\theta}$, then

$$Z_e = |V|\phi\chi_0 e^{j(\theta - 2\zeta)} . \tag{91}$$

The procedure for determining Z_e from the equivalent circuit of Fig. 9 can be summarized as follows:

1. Follow steps 1, 2, and 3 that were listed for the efficiency analysis.

2. Calculate the values of the blocked mechanical mobility for the particular frequency and ratio of f to f_c^s. Input these values into the ac-circuit analysis program.

3. Record the magnitude $|V|$ and phase θ of the input (node 1, Fig. 9) velocity. Use Eq. (91) to calculate Z_e.

4. To calculate Z_e at another frequency, return to step 1. Notice that three circuit elements must be changed for each frequency point. These are the two blocked mechanical mobilities and the force generator.

The transmitting voltage response is obtained as follows:

1. Follow steps 1 and 2 of the procedure just summarized for calculating Z_e.

2. Record the magnitude $|V|$ of the input velocity (node 1, Fig. 9), and use the following equation to calculate the input voltage:

$$|e| = \text{magnitude of the voltage} = |V|\phi\chi_0. \tag{92}$$

3. Calculate the power dissipated in the radiation mobility ($1/A^2R_A$) for the input voltage of step 2. Use Eq. (85) to calculate the on-axis acoustic pressure and divide this pressure by the result of Eq. (92).

The equivalent circuit of Fig. 9 is based on an exact eddy-current theory that will work at any frequency subject to the assumptions under which the circuit was derived. But the wide frequency range of the equivalent circuit of Fig. 9 is a tradeoff with the complexity of the analysis required to obtain results. It would be desirable to have an equivalent circuit that has lumped components, that is, with none of the elements (capacitors, resistors, inductors, or current generator) changing with frequency. Such an equivalent circuit is possible over a limited frequency range and will be described in the succeeding paragraphs.

To derive a lumped equivalent circuit, one must approximate the eddy current factor χ in such a way that the frequency-dependent elements of Fig. 7 become a combination of frequency-independent elements. This has already been accomplished for the blocked impedance (branch 2) of Fig. 7. When $f/f_c^s \leq 2$, the blocked impedance (for a circularly cross-sectioned core) of Fig. 7 can be represented quite accurately by Fig. 4, where L_0 is given by Eq. (55) and f_c^s is given by Eq. (81). Figure 4 was derived by assuming $\chi_R \approx 1$ and $\chi_I \approx f/8f_c^s$, which implies that

$$\chi = \chi_R - j\chi_I \tag{93}$$

$$\approx 1 - j\frac{f}{8f_c^s} \tag{94}$$

for $f/f_c^s < 2$. Therefore branch 3 of Fig. 7 becomes

$$j\omega C_m \phi^2 \chi^2 \approx j\omega C_m \phi^2 \left[1 - 2j\frac{f}{8f_c^s} - \frac{f^2}{64\left(f_c^s\right)^2}\right] \tag{95}$$

$$\approx j\omega C_m \phi^2 + \frac{\pi f^2 C_m \phi^2}{2f_c^s}\ , \tag{96}$$

if the last term of Eq. (95) is neglected. Equation (96) can be written in an equivalent parallel representation shown in Fig. 10. Figure 10 is the lumped form which is desired. Branch 4 in Fig. 7 becomes

$$\frac{\chi^2 \phi^2}{j\omega M_m} \approx \frac{1 - 2j\dfrac{f}{8f_c^s} - \dfrac{f^2}{64\left(f_c^s\right)^2}}{j\omega \dfrac{M_m}{\phi^2}} \tag{97}$$

$$= \frac{1}{j\omega \dfrac{M_m}{\phi^2}} - \frac{1}{8\pi f_c^s \dfrac{M_m}{\phi^2}} + \frac{j\omega}{\left(16\pi f_c^s\right)^2 \dfrac{M_m}{\phi^2}}\ . \tag{98}$$

Equation (98) can be represented by Fig. 11. Branch 5 in Fig. 7 becomes

$$\frac{\phi^2 \chi^2}{R_m} \approx \frac{\phi^2}{R_m}\left(1 - j\frac{f}{4f_c^s}\right) \tag{99}$$

$$= \frac{\phi^2}{R_m} + j\omega\left(\frac{-1}{8\pi f_c^s \dfrac{R_m}{\phi^2}}\right)\ . \tag{100}$$

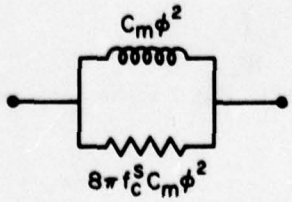

Fig. 10 — Approximate equivalent circuit of the mechanical compliance in the presence of small eddy currents

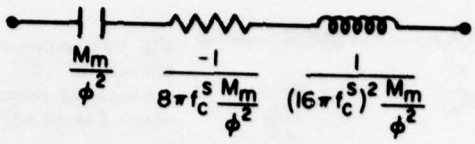

Fig. 11 — Approximate equivalent circuit of the mechanical mass in the presence of small eddy currents

Equation (100) can be represented by Fig. 12. Branches 6 and 7 are represented similarly. The resulting lumped equivalent circuit of a magnetostrictive toroid (with a circular-cross-section core) in the presence of eddy currents ($f/f_c^s \leq 2$) is shown in Fig. 13. Figure 13 has nine nodes and 15 branches compared with three nodes and seven branches for the equivalent circuit without eddy currents. Figure 13 is in electrical units. The efficiency of a transducer described by Fig. 13 is obtained by analyzing the circuit with an ac-network routine. The power dissipated in the resistances of Fig. 13 is

$$P = \frac{e^2}{R}, \tag{101}$$

where e is the branch voltage and R is the branch resistance. The power dissipated by eddy currents is that dissipated in branches 3, 4, 7, and 14. The power dissipated in the negative resistances of branches 7 and 14 must be interpreted as negative power in order to obtain correct results. The mechanical dissipation occurs in branch 9, and the acoustical dissipation occurs in branch 11. The efficiency is given by Eq. (84). As eddy currents become small, f_c^s approaches infinity, which means that the elements of Fig. 13 approach those of the equivalent circuit without eddy currents.

The transmitting current response is calculated from Eq. (85) using the power dissipated in branch 11 for a 1-ampere current generator. The electrical impedance is calculated from the quotient of the complex voltage at node 1 and the value of the current generator. The transmitting voltage response is computed from the power dissipated in branch 11 and the driving voltage at node 1.

An equivalent circuit similar to Fig. 13 can be derived for a magnetostrictive toroid with a core composed of thin sheets in the presence of small eddy currents. In the case of a thin-sheet core the eddy current factor χ becomes

$$\chi = \chi_R - j\chi_I \tag{102}$$

$$\approx 1 - j\frac{f}{3f_c^s}, \tag{103}$$

where f_c^s is given by Eq. (82). Applying Eq. (103) to Fig. 7 yields the desired equivalent circuit (Fig. 14).

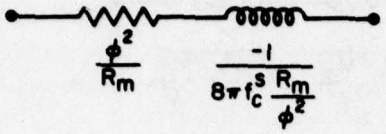

Fig. 12 — Approximate equivalent circuit of the inverse of the mechanical resistance in the presence of small eddy currents

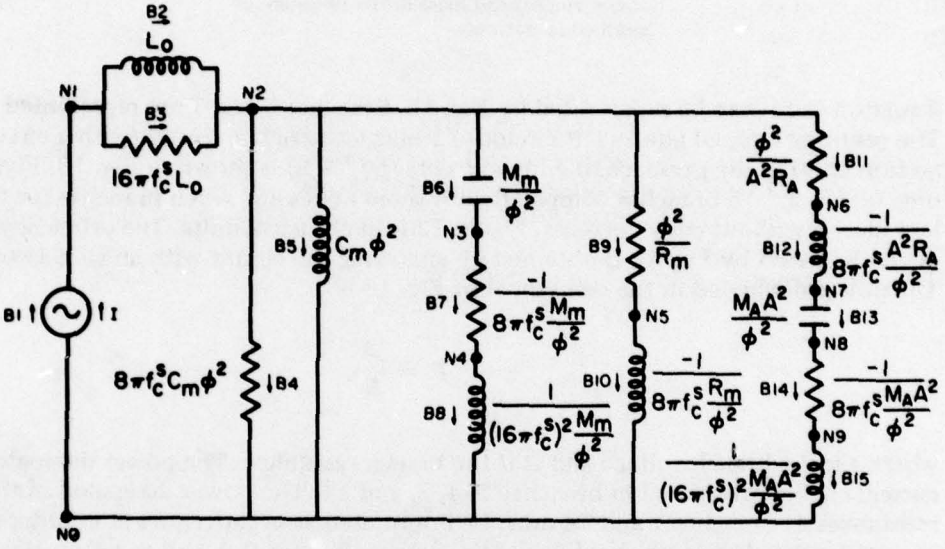

Fig. 13 — The equivalent circuit of a magnetostrictive toroid with a circular-cross-section core in the presence of small eddy currents

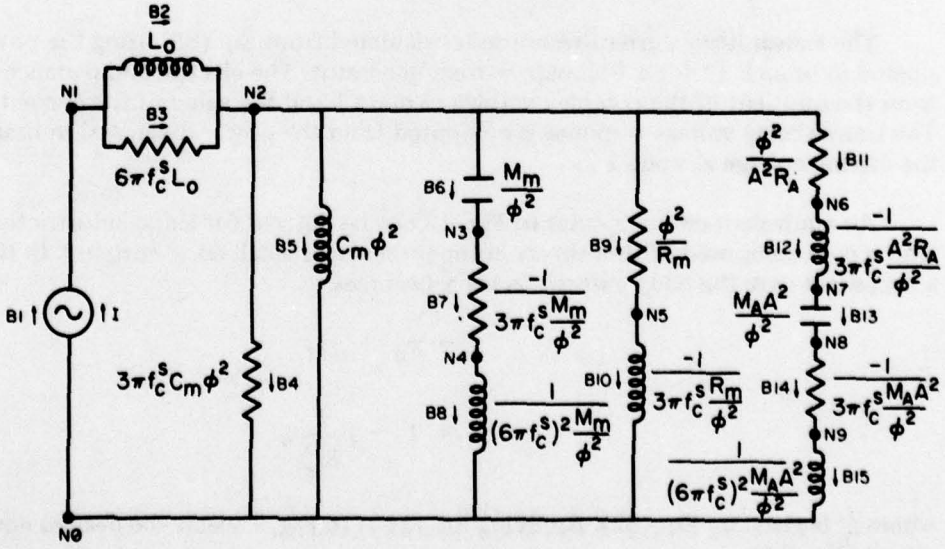

Fig. 14 — The equivalent circuit of a magnetostrictive toroid with a core composed of thin sheets in the presence of small eddy currents

Results and Discussion of Equivalent Circuits

Figure 15 shows the electroacoustic efficiency in decibels versus normalized frequency and f/f_c^s for a toroid with a circular cross section. This figure was generated from Figs. 13 and 9 for the small-eddy-current approximation and the exact eddy-current theory respectively. Below $f/f_c^s = 1$ the exact and approximate theory are in excellent agreement. The difference between the exact and approximate theory does not reach 1 dB until $f/f_c^s = 2.3$. The point of maximum efficiency need not occur at the point of maximum power output $f/f_r = 1$, since here maximum efficiency occurs at $f/f_r = 1.3$.

Figure 16 shows the electroacoustic efficiency in decibels versus normalized frequency and f/f_c^s for a toroid with a core composed of thin sheets. This graph was generated from Figs. 14 and 9 for the small-eddy-current approximation and the exact eddy-current theory respectively. The agreement between the exact and approximate theories is not as good here as in Fig. 15. There is a 1-dB difference at $f/f_c^s = 0.75$ and 1.7-dB difference at $f/f_c^s = 1.0$. Therefore the use of Fig. 14 for efficiency calculations should be limited to ratios of f to f_c^s below unity. The predictions of Figs. 13 and 14 yield a greater value of efficiency than would be measured.

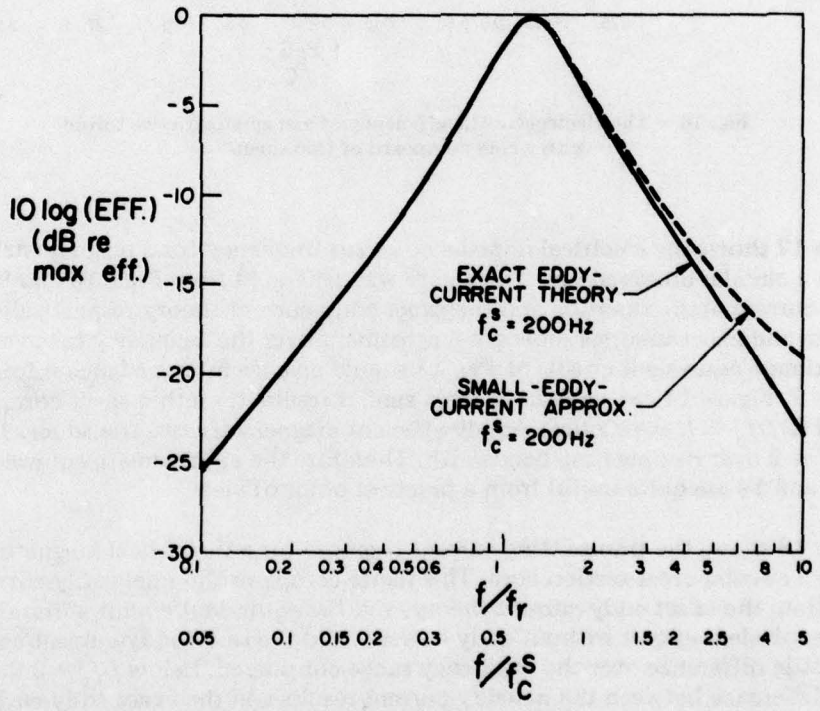

Fig. 15 — The electroacoustic efficiency of a magnetostrictive toroid with a circular cross section

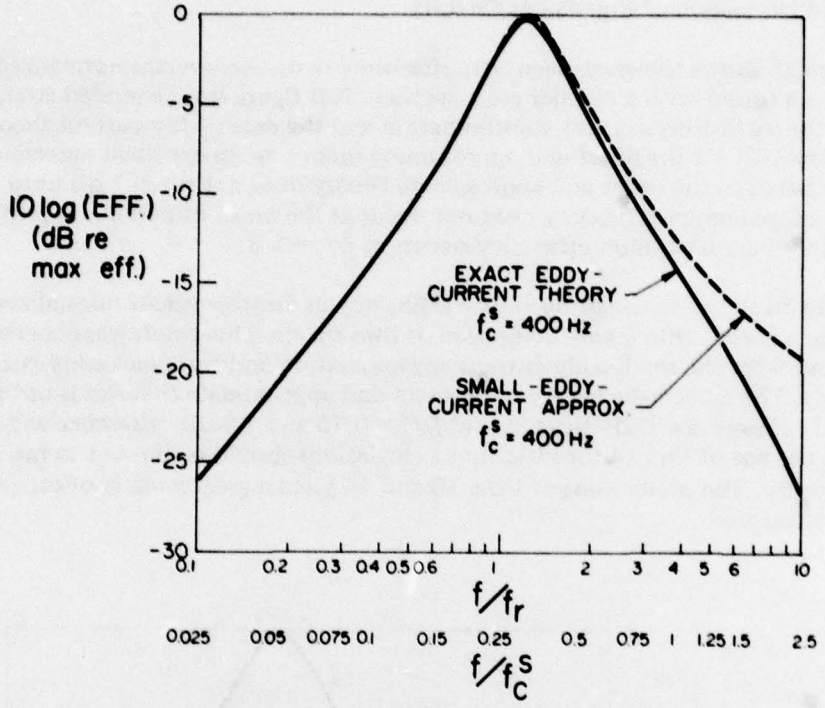

Fig. 16 — The electroacoustic efficiency of a magnetostrictive toroid with a core composed of thin sheets

Figure 17 shows the electrical impedance versus frequency for a magnetostrictive toroid with a circular cross section. This figure was generated from Figs. 13 and 9 for the small-eddy-current approximation and the exact eddy-current theory respectively. The approximate and exact theories show good agreement over the frequency range covered. The approximate equivalent circuit of Fig. 13 should give useful impedance information up to $f/f_c^s = 2$. Figure 14 can be used to yield similar results for a thin-sheet core, although it is limited to $f/f_c^s \leq 1$. A practical, highly efficient magnetostrictive transducer is designed so that $f/f_c^s \leq 2$ over its operating bandwidth. Therefore the approximate equivalent circuits of Figs. 13 and 14 are quite useful from a practical point of view.

Figure 18 shows the transmitting current response for a theoretical magnetostrictive toroid with a circular-cross-section core. This figure compares the small-eddy-current approximation, the exact eddy-current theory, and the equivalent circuit without eddy currents. The equivalent circuit without eddy currents and the small-eddy-current approximation show little difference over the frequency range considered. Below $f/f_c^s = 2$ there is less than 1-dB difference between the no-eddy-current results and the exact eddy-current theory. Therefore, to calculate the transmitting current response at frequency ratios below $f/f_c^s = 2$, one need use only the equivalent circuit without eddy current loss or the small-eddy-current approximation, since there is little difference between them. Above $f/f_c^s = 2$ one should use the exact eddy-current theory.

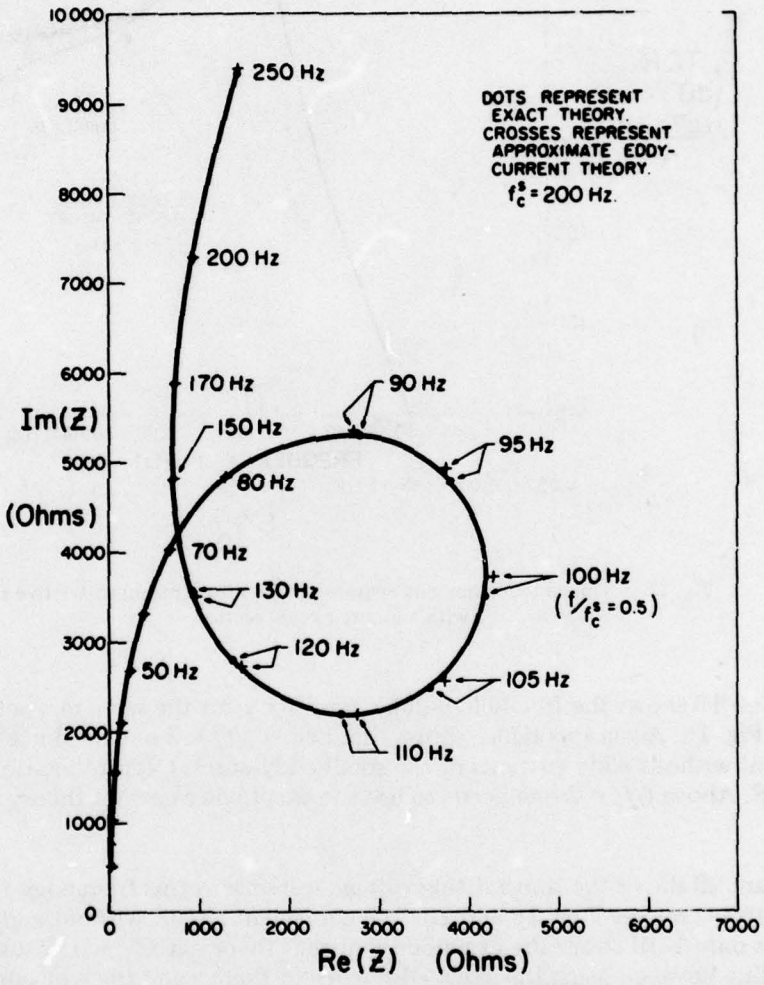

Fig. 17 — The electrical impedance versus frequency for a magnetostrictive toroid with a circular cross section

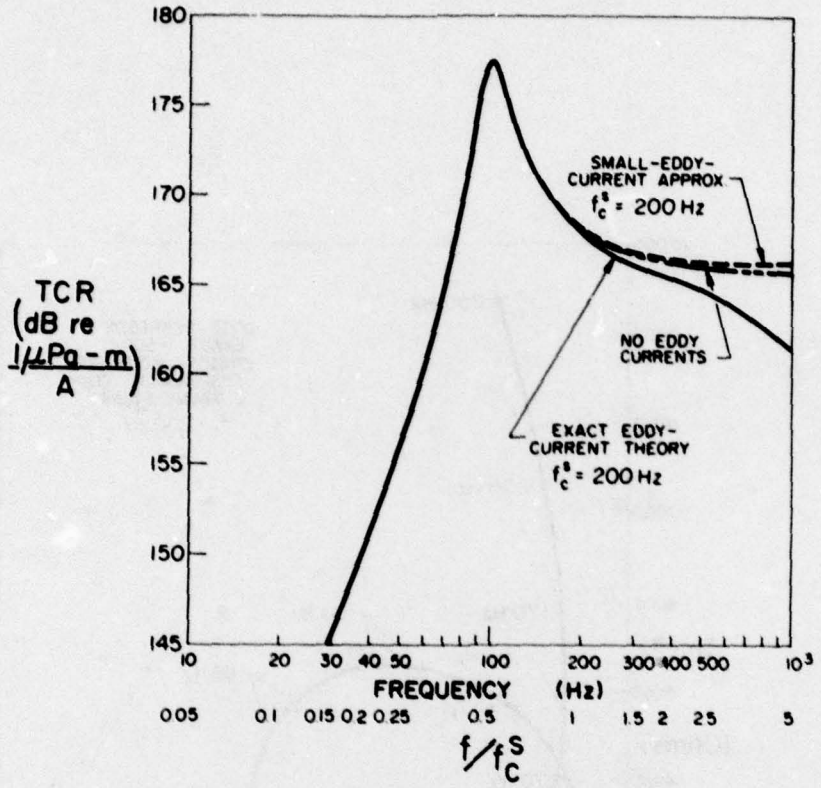

Fig. 18 — Transmitting current response (TCR) for a magnetostrictive toroid with a circular cross section

Figure 19 shows the free-field voltage sensitivity for the same magnetostrictive transducer as Fig. 18. Again this figure shows that below $f/f_c^s = 2$ one need use only the equivalent circuit without eddy currents or the small-eddy-current approximation to calculate the FFVS. Above $f/f_c^s = 2$ one needs to use the exact eddy-current theory to obtain good results.

Figure 20 shows the transmitting voltage response versus frequency for the same magnetostrictive toroid as Figs. 18 and 19. The equivalent circuit without eddy current loss (Fig. 6) is only 1 dB above the exact eddy-current theory at $f/f_c^s = 3$. Thus $f/f_c^s = 3$ is the dividing line between using the exact eddy-current theory and the equivalent circuit without eddy current loss. In this case the small-eddy-current approximation is not quite as good as the results obtained from the equivalent circuit without eddy currents.

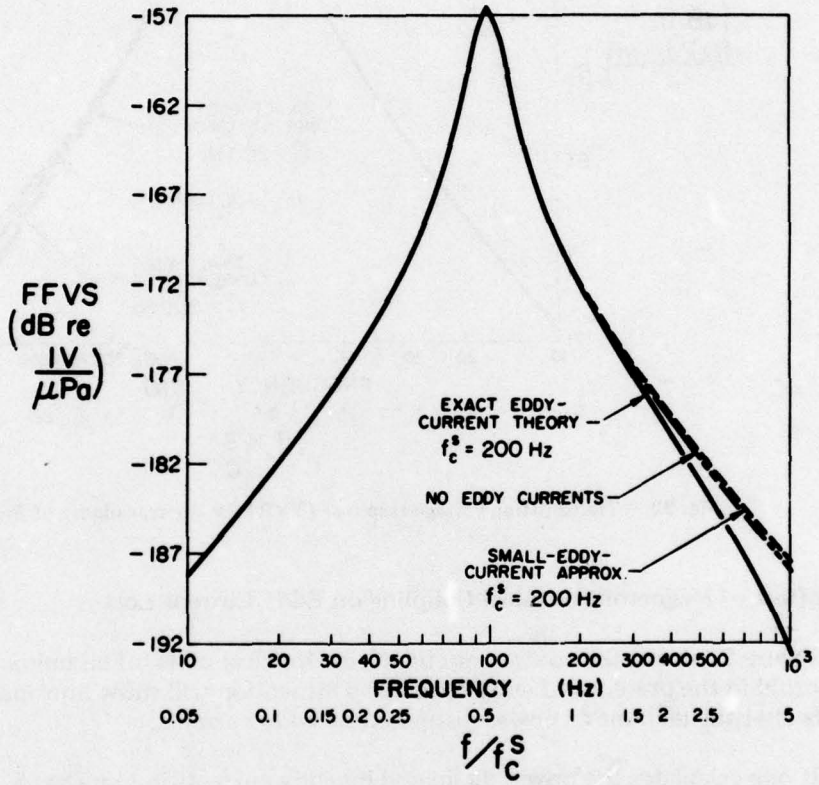

Fig. 19 — Free-field voltage sensitivity (FFVS) for the transducer of Fig. 18

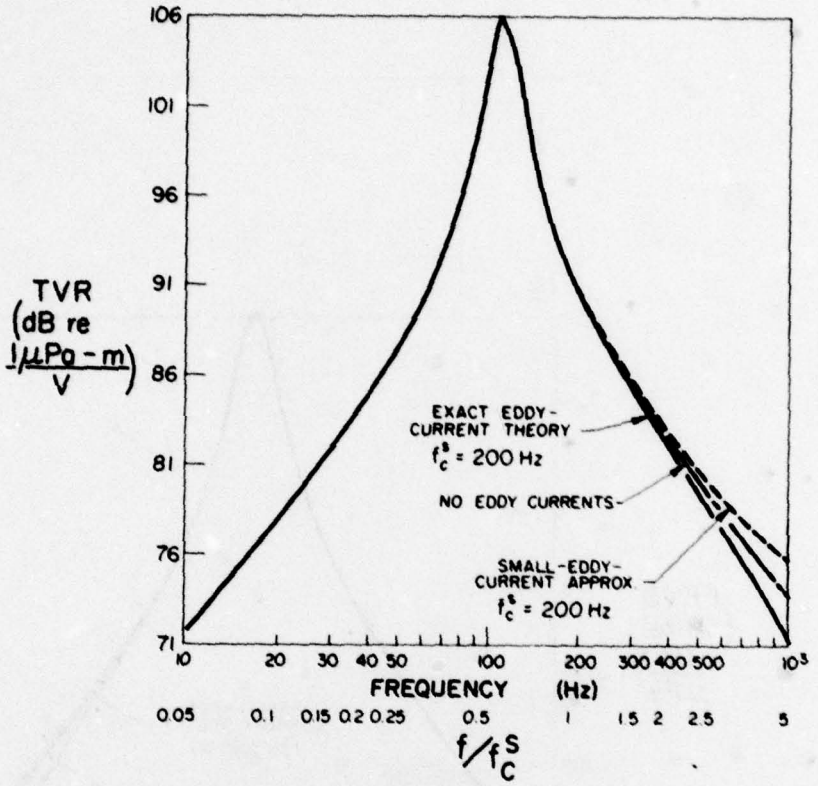

Fig. 20 — Transmitting voltage response (TVR) for the transducer of Fig. 18

The Effect of Magnetomechanical Coupling on Eddy Current Loss

Figure 21 shows the equivalent circuit, in electrical units, of an unloaded magnetostrictive toroid in the presence of eddy currents. This section will show how magnetoelastic effects alter the amount of power dissipated by eddy currents.

If one calculates the power dissipated by eddy currents in branches 2, 3, and 4 (no eddy current power being dissipated in branch 5, only mechanical power), the following equation results:

$$P_{\text{eddy}}(\omega) = I^2 \omega L_0 \chi_I \left[1 + \frac{2\chi_R k_{33}^2 - 2\chi_R k_{33}^2 \dfrac{\omega^2}{\omega_0^2}}{\left\{ \left(1 - \dfrac{\omega^2}{\omega_0^2}\right)^2 + \dfrac{\omega^2}{\omega_d^2} \right\} \left(1 - k_{33}^2\right)} \right], \tag{104}$$

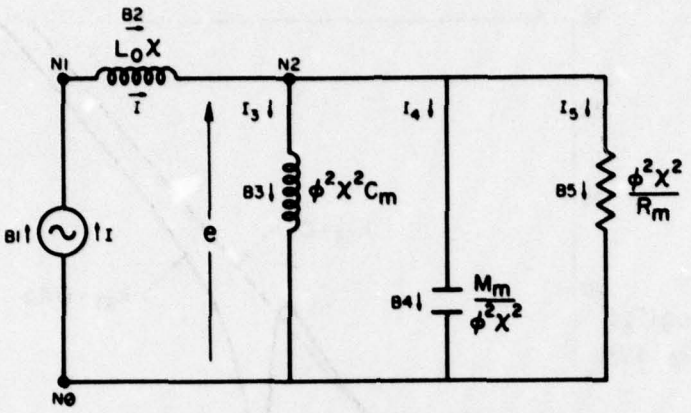

Fig. 21 — The equivalent circuit, in electrical units, of an unloaded magnetostrictive toroid in the presence of eddy currents

where

$$\omega_0^2 = \frac{1}{C_m M_m} \tag{105}$$

and

$$\omega_d^2 = \frac{1}{C_m^2 R_m^2}. \tag{106}$$

The frequencies ω_0 and ω_d are the resonance frequency and a damping frequency respectively. Equation (106) implies that as the mechanical damping R_m approaches zero, the damping frequency approaches infinity. The result of using the small-eddy-current approximations of Eq. (94) in Eq. (104) is

$$P_{\text{eddy}}(\omega) \approx \frac{I^2\omega^2 L_0}{16\pi f_c^s} + \frac{I^2\omega^2 L_0 2k_{33}^2 - I^2\frac{\omega^4}{\omega_0^2}L_0 2k_{33}^2}{16\pi f_c^s(1-k_{33}^2)\left\{\left(1-\frac{\omega^2}{\omega^2}\right)^2 + \frac{\omega^2}{\omega_d^2}\right\}} \tag{107}$$

Equation (107) is plotted in Fig. 22 for $L_0 = 6.45$ H, $f_c^s = 1000$ Hz, $k_{33} = 0.45$, $\omega_0 = (2\pi)100$ Hz, and $\omega_d = (2\pi)389$ Hz. Also shown in Fig. 23 is the eddy current loss for a nonmagnetostrictive toroid ($k_{33} = 0$) that has a permeability equal to μ_{33} (the free permeability). When $\omega << \omega_0$, the two curves converge. This can be seen from Eq. (107) by letting $\omega << \omega_0$:

$$P_{\text{eddy}}(\omega) = \frac{I^2\omega^2 L(1+k_{33}^2)}{16\pi f_c^s(1-k_{33}^2)}. \tag{108}$$

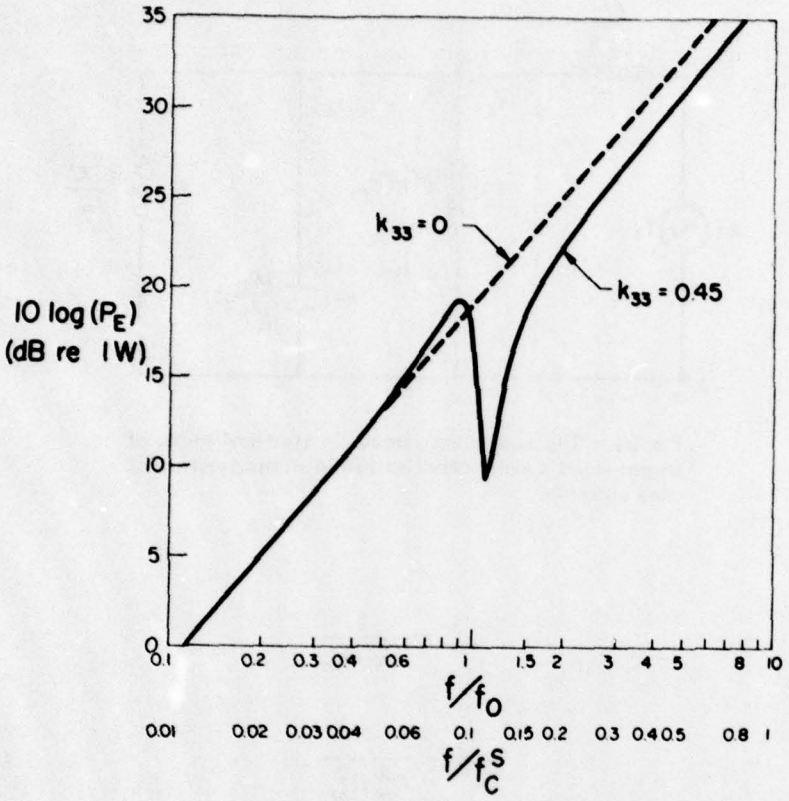

Fig. 22 — The power dissipated by eddy currents as a function of frequency when $k_{33} = 0.45$

Let

$$L_T = \text{free inductance} = \frac{L_0}{1 - k_{33}^2} \tag{109}$$

and

$$f_c^T = \frac{2\rho}{\pi d^2 \mu_{33}^T} = f_c^s(1 - k_{33}^2) = \text{free characteristic frequency.} \tag{110}$$

Thus Eq. (108) becomes

$$P_{\text{eddy}}(\omega) = \frac{I^2\omega^2 L_T(1 - k_{33}^4)}{16\pi f_c^T} \approx \frac{I^2\omega^2 L_T}{16\pi f_c^T} \quad . \tag{111}$$

Equation (111) is the same as the expression for the eddy current loss of a nonmagnetostrictive toroid with permeability μ_{33}^T for $f < f_c^T$. Equation (111) means that at frequencies far

below resonance (where the motional impedance is small) the power lost in eddy currents of a magnetostrictive toroid is the same as in a nonmagnetostrictive toroid with permeability $\mu = \mu_{33}^T$. When $\omega = \omega_0$, Eq. (107) becomes

$$P_{\text{eddy}}(\omega_0) = \frac{I^2 \omega_0^2 L_0}{16\pi f_c^s}. \tag{112}$$

Equation (112) is the same as the expression for the loss of a nonmagnetostrictive toroid with permeability $\mu = \mu_{33}^S$ at $\omega = \omega_0$ and $f < f_c^s$. When $\omega >> \omega_0$, Eq. (107) becomes

$$P_{\text{eddy}}(\omega) = \frac{I^2 \omega^2 L_T (1 - k_{33}^2)^2}{16\pi f_c^T} = \frac{I^2 \omega^2 L_0}{16\pi f_c^s}, \tag{113}$$

which is the same as Eq. (112) except that ω has replaced ω_0. Equation (113) means that far above resonance the $k_{33}^2 = 0.45$ curve of Fig. 22 is less than the $k_{33} = 0$ curve by a factor of $(1 - k_{33}^2)^2$.

The most interesting phenomenon shown in Fig. 22 is the 10-dB drop below the $k_{33} = 0$ curve in the eddy current loss at $f/f_0 = 1.11$, just past the resonance frequency. Savage and Abbundi [10] have observed this effect experimentally. This present theory explains that effect. Physically this drop in the eddy current power dissipated means that the skin depth of the magnetostrictive material increases over a narrow frequency range just above the resonance frequency. It has been found that the depth of the minimum at $f/f_0 = 1.11$ is controlled by both the damping frequency ω_d and the coupling coefficient k_{33}. The damping frequency is related to the mechanical resistance R_m via Eq. (106). A small mechanical damping (large ω_d) leads to a great drop in the eddy current loss just past ω_0. A large mechanical damping (small ω_d) leads to a shallow drop in the eddy current power above resonance. The occurance of such a drop in eddy current loss could lead to a dramatic rise in the efficiency of a transducer that has a large portion of its loss in eddy current ohmic loss.

Figure 23 shows the eddy current power dissipated as a function of frequency for $L_0 = 7.36$ H, $f_c^s = 1000$ Hz, $k_{33} = 0.3$, $\omega_0 = (2\pi)100$ Hz, and $\omega_d = (2\pi)875$ Hz. The reduced coupling coefficient moves both the maximum and the minimum closer to f_0. The maximum and minimum occur at $0.95\, f_0$ and $1.055\, f_0$ respectively. The difference between the curves above resonance is less than that in Fig. 22. This is expected in light of Eq. (113).

Extension of the Small-Eddy-Current Approximations to Additional Equivalent Circuits

The only equivalent circuit discussed so far has been that of a magnetostrictive toroid. The small-eddy-current approximations presented in Figs. 13 and 14 apply to any magnetostrictive device with an active core that is circular in cross section or composed of a stack of thin sheets. Figure 24 shows an example in which the approximations of Fig. 13 have been

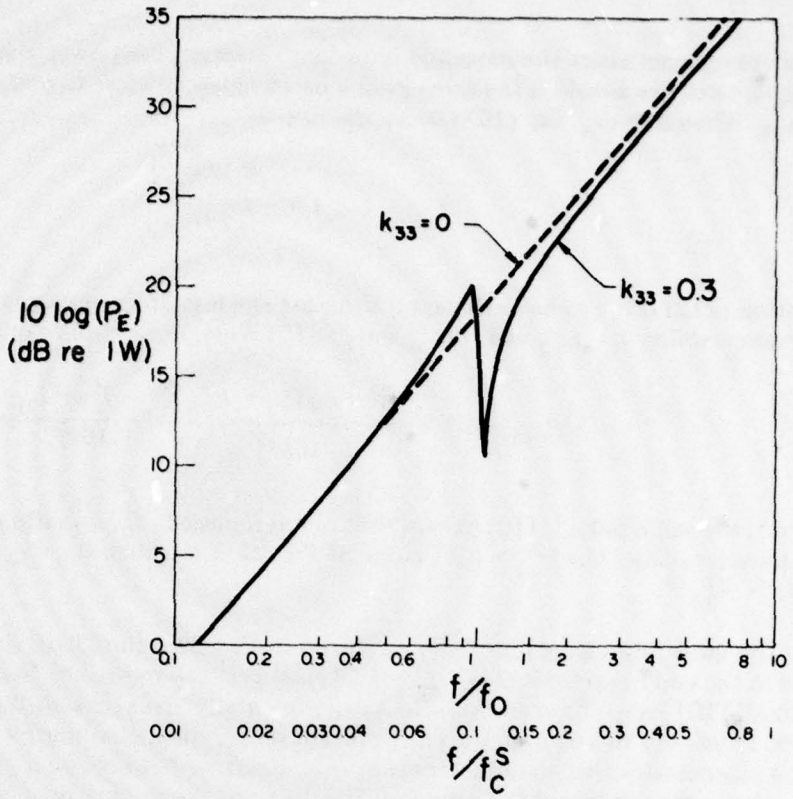

Fig. 23 — The power dissipated by eddy currents as a function of frequency when $k_{33} = 0.3$

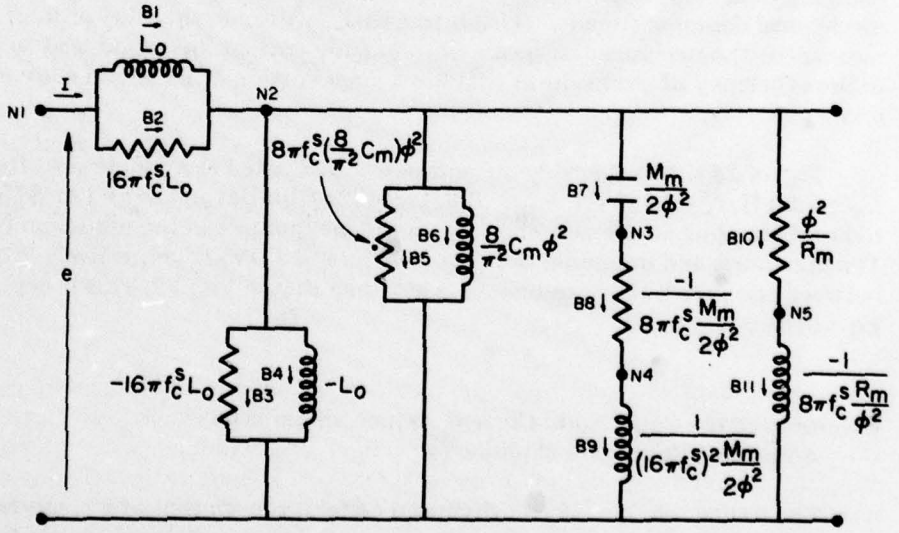

Fig. 24 — The equivalent circuit of a circular magnetostrictive rod clamped at one end in the presence of small eddy currents near its quarter-wave resonance

applied to the equivalent circuit of a thin magnetostrictive rod of circular cross section with one end clamped. Branches 1 through 4 are the blocked impedance. Branches 5 through 9 are Mason's approximations to the mechanical admittance with the approximations of Fig. 13 applied. Branches 10 and 11 are the reciprocal of the mechanical resistance with the small-eddy-current approximation applied. In Fig. 24 the constants are given by

$$L_0 = \frac{N^2 A \mu_{33}^S}{\ell}, \tag{114}$$

$$\phi = \frac{N d_{33} A}{s_{33}^H \ell}, \tag{115}$$

$$C_m = \frac{s_{33}^B \ell}{A}, \tag{116}$$

$$M_m = DA\ell, \tag{117}$$

and

$$R_m = \frac{\omega_0 M_m}{2Q_m}, \tag{118}$$

where ℓ is the length of the rod, A is its cross-sectional area, and D is its density, all in SI units. Several restrictions apply to Fig. 24:

- One end of the rod is rigidly clamped, and the other end is free to move;
- The frequency is near the quarter-wave resonance of the rod;
- The rod is long and thin, so that any demagnetizing effects are small, or equivalently a well-laminated low-reluctance magnetic return path is provided;
- The frequency range of interest is less than or equal to twice the clamped characteristic frequency (f_c^s).

SUMMARY AND CONCLUSIONS

The equivalent circuit of a magnetostrictive transducer in the presence of eddy currents has been derived using an exact eddy-current theory. The exact eddy-current theory can be time consuming to use but can be reduced to an approximate theory which is simple and accurate for frequency ranges of practical interest. The approximate eddy-current theory is useful in predicting the efficiency, the impedance, the transmitting responses, and the receiving response in a range of frequencies near the clamped characteristic frequency f_c^s. At

frequencies greater than twice the characteristic frequency the exact eddy-current theory will yield accurate results. The approximate eddy-current theory should have immediate application by transducer designers working with magnetostrictive transducers.

It was found that the eddy current theory predicted a sharp drop in the eddy-current loss in a narrow frequency range just past resonance. This effect was experimentally observed by Savage and Abbundi [10].

REFERENCES

1. K.L. Scott, Proceedings of the IRE 18, 1750-1764 (Oct. 1930).
2. M. Abramowitz and I.A. Stegun, editors, *Handbook of Mathematical Functions*, Dover, New York, 1972, p. 430.
3. R.M. Bozorth, *Ferromagnetism*, Van Nostrand, New York, 1951, Chapter 17.
4. "The Design and Construction of Magnetostriction Transducers," Summary Technical Report of Division 6, National Defense Research Committee, Washington, D.C., 1946, Vol. 13, Chapter 3.
5. G.R. Slemon, *Magnetoelectric Devices*, Wiley, New York, 1966, p. 121.
6. T.F. Hueter and R.H. Bolt, *Sonics*, Wiley, New York, 1955, Chapter 5.
7. F.V. Hunt, *Electroacoustics*, Harvard University Press, Cambridge, Mass., and Wiley, New York, 1954, Chapters 3, 4, and 7.
8. S. Hart, *AC Circuit Analysis Program*, Digital Equipment Corporation, Maynard, Mass., Decus 11-12, Mar. 8, 1971.
9. R.J. Bobber, *Underwater Electroacoustic Measurements*, U.S. Government Printing Office, Washington, D.C., 1970, Chapters 2 and 3.
10. H.T. Savage and R. Abbundi, IEEE Transactions on Magnetics 14, 545 (Sept. 1978).